Journal of Mathematical Modeling and Fractional Calculus
https://acspublisher.com/journals/index.php/jmmfc
Received:08-11-2024, **Revised:** 05-12-2024,
Accepted:10-12-2024, **Published:** 31-12-2024,
https://doi.org/10.48165/jmmfc.2024.1202, 1(2),23-39.

Modeling and Stability Analysis of the Unemployment Model with Caputo Derivative

Saba Jamil[a], Khadija Jamil[a], Aamir Shehzad[b]

[a]Institute of Mathematics, Khwaja Fareed University of Engineering and Information Technology, Pakistan.
[b]Mathematical Research Center, Near East University, Turkey.
Corresponding author Email: saba.jamil@kfueit.edu.pk

Abstract:
The problem of unemployment is acute, joblessness affects millions of people worldwide, which is why governments are constantly looking for efficient solutions to combat this social and economic ill. In response, we construct a model that encompasses the nonlinear nature of the unemployment rate. A fractional-order system of differential equations is employed in the structure of the considered model to produce a more accurate analysis of the unemployment dynamics of equilibrium positions and their stability or instability. In the model, there are three main dynamical parameters whose time evolution is described by fractional-order differential equations involving Caputo derivatives. The existence and uniqueness of the solutions are established by using the fixed point indices and the stability of the model is determined by applying the Hyers-Ulam stability test. A Newton polynomial approach is used for numerical simulation and investigates the results at fractional orders $\omega = 0.85 \textit{ and } \omega = 1$. The results presented in this paper suggest that there is one and only one stable positive equilibrium that is locally and globally asymptotically stable under some conditions. Computations demonstrate that for different values of ω, obtained with Caputo derivatives coinciding with the classical sense at $\omega = 1$. In this study, by determining the employment rate and job creation rate that produce an unemployment rate of 7% the model complies with the governments policy objectives of low unemployment. These results provide important implications for the dynamic employment policies suggested and point to the use of fractional-order methodologies in other economic-social systems.

Keywords: Unemployment, Stability, Numerical simulation, Caputo operator.

1. Introduction

Unemployment is a major issue impacting individuals, communities, and nations worldwide. It refers to the condition where individuals actively seeking employment, despite meeting specific qualifications, are unable to secure jobs that match their skills. High unemployment rates have far-reaching consequences, including economic uncertainty, social inequality, and psychological distress [1]. In society, unemployment is particularly destructive as it fosters social issues such as rejection, reduced self-esteem, and depression among affected individuals [2]. It exacerbates disparities, especially among youth and other vulnerable groups, undermining equality and deepening divisions. Additionally, unemployment is linked to increased crime rates and potential social instability, posing significant barriers to the smooth functioning of society and human well-being [3, 4, 5]. The study [6] employs mathematical modeling to analyze and predict unemployment trends while exploring strategies to mitigate

the effects of rising unemployment rates.
Mathematical modeling is a powerful tool for analyzing and predicting unemployment trends while evaluating the effects of various policy measures. By capturing the complexities of unemployment dynamics, these models enable researchers and policymakers to understand underlying mechanisms, identify critical influencing factors, and explore effective strategies for mitigating unemployments negative impacts. Recent studies have increasingly focused on mathematical approaches to unemployment modeling [7, 9, 10]. Al-Maalwi et al. [7] emphasized that to prevent rising unemployment, job creation must meet or exceed the equilibrium unemployment level. Similarly, Sheikh et al. [8] and Al-Maalwi et al. [10] highlighted the significant role communities can play in reducing unemployment, particularly when government job-creation efforts fall short.
The Atangana derivative has been recognized for its efficient memory operator, characterized by non-local and non-singular kernel properties [10]. Fractional operators have proven highly effective in modeling complex physical processes with exceptional accuracy. For instance, the study in [11] applied a Caputo fractional derivative to analyze the dynamics of social media addiction. Similarly, [12] explored unemployment dynamics using the fractional power law and the Mittag-Leffler function. Jamil et al. (2024) in [13] conducted an in-depth analysis of respiratory syncytial virus (RSV) infections through a fractional-order mathematical model. The authors in [14] provided a comprehensive examination of Hepatitis B Virus (HBV) dynamics, incorporating vaccination and treatment strategies via a novel fractional derivative approach. Additionally, [15] investigated COVID-19 transmission dynamics using a fractional-order framework that included age dependence, while [16] presented an advanced mathematical model to study the dynamics of Ebola virus epidemics.
Our study employs fractional-order derivatives due to their ability to incorporate memory effects, capturing both cumulative and delayed influences on unemployment dynamics. Unlike integer-order models, which account only for instantaneous changes, fractional calculus considers historical factors such as past policies and economic conditions. This approach provides valuable insights into past dependencies, with unemployment rates demonstrating sensitivity to historical job creation rates (σ). Fractional models also facilitate smoother transitions between unemployment states, closely aligning with real-world dynamics. These features make the fractional model a powerful tool for shaping policies that address both immediate and long-term socio-economic challenges. The article begins with an introduction in Section 1, followed by preliminary fractional-order derivatives that provide foundational understanding of unemployment dynamics in Section 2. In Section 3, we present the proposed model, determine the equilibrium state, and discuss its local stability. Section 4 confirms the existence and uniqueness of solutions using the fixed-point approach, while Section 5 applies non-linear analysis to establish Ulam-Hyers stability. An advanced numerical method is introduced in Section 6 to solve the fractional-order system and verify the impact of fractional parameters. The findings are discussed in detail in Section 7, with the study concluding in Section 8.

2. Fundamental Concepts

This portion consists of some fundamental ideas that are useful for system analysis.

Definition 2.1. *[11] The usual Caputo time-fractional derivative of order ν is expressed as*

$$^{C}D_t^{\varepsilon} z(t) = \frac{1}{\Gamma(1-\varepsilon)} \int_0^t (t-\rho)^{-\varepsilon} z'(\rho) d\rho, 0 \leq \varepsilon \leq 1.$$

Definition 2.2. *[11] The corresponding fractional integral operator $\varepsilon \in (0,1)$ for Caputo FD is as follows:*

$$^{\mathtt{C}}I_t^{\varepsilon}\Big(z(t)\Big) = \frac{1}{\Gamma(\varepsilon)} \int_0^t (t-\rho)^{\varepsilon-1} z(\rho) d\rho.$$

3. Unemployment Fractional Order Model

In the model formation process, we assume that all the people who are categorized as unemployed have the skills and /or qualifications to be employed. The unemployed people population U(t) increases by A with time. Employment of these people may be occasioned by the obtaining of a certain employment rate K which may affect the employment people, denoted as E(t). However, some of the employed will lose their jobs or quit their jobs to join the unemployed list at a certain rate. The unemployed die or migrate in proportion to their quantities and every employed worker migrates, retires, or dies at the rate of α. The available job vacancies at a given time, V(t), are generally offered by both the Government and private organizations, and; it is taken that the number of those willing to work is in direct proportion with the unemployed persons at a ratio of σ. The Quicker steeled employment empty position probabilities that an unemployed person enters vacancies, is directly associated with the number of unemployed and vacancies increased at a rate of K. The rate at which vacancies are eliminated because of the deficiency of government funding; The rate of government funding is inadequate concerning shortages δ.

$$\begin{aligned}
&{}_0^cD_t^{\omega}U(t) = A - KU(t)V(t) + \beta E(t) - \mu U(t). \\
&{}_0^cD_t^{\omega}E(t) = KU(t)V(t) - \beta E(t) - \alpha E(t). \\
&{}_0^cD_t^{\omega}V(t) = \sigma U(t) - \delta V(t).
\end{aligned} \tag{1}$$

3.1. Equilibrium Point and Local Stability

To find the equilibrium points of the system (1), we put the left-hand side of the system (1) as zero. Consequently, by direct calculations, it is possible to state the fact that there is only one positive equilibrium point denoted as I* $= (U^*, E^*, V^*)$ where

$$V^* = \frac{\sigma U^*}{\delta},$$

$$E^* = \frac{K\sigma U^{*2}}{\delta(\alpha+\beta)},$$

$$U^* = \frac{-(\alpha+\beta)\delta\mu + \sqrt{[(\alpha+\beta)\delta\mu]^2 + 4(K\sigma\alpha)((\alpha+\beta)\delta)}}{2K\sigma\alpha}.$$

Theorem.3.1 The positive equilibrium I* $= (U^*, E^*, V^*)$ is locally asymptotically stable.
Proof Evaluating system (1) Jacobian matrix at positive equilibrium I* gives

$$J(\mathrm{I}^*) = \begin{pmatrix} -KV^* - \mu U^* & \beta & -KU^*, \\ KV^* & -\beta - \alpha & KU^*, \\ \sigma & 0 & -\delta \end{pmatrix},$$

$$= \begin{pmatrix} -kV^* - \mu U^* - \lambda & \beta & -kU^* \\ kV^* & -(\alpha+\beta) - \lambda & kU^* \\ \sigma & 0 & -\delta - \lambda \end{pmatrix}$$

$$\begin{aligned}
&= (-kV^* - \mu U^* - \lambda)[(-(\alpha+\beta) - \lambda)(-\delta - \lambda)] - \beta[-(\delta+\lambda)(\mathrm{K}V^*) - \sigma(\mathrm{K}U^*)] \\
&-\mathrm{K}U^*(\sigma(\alpha+\beta+\lambda)),
\end{aligned}$$

$$\begin{aligned}
&= (-kV^* - \mu U^* - \lambda)\left[\alpha\delta + \beta\delta + \lambda\delta + \alpha\lambda + \beta\lambda + \lambda^2\right] - \beta[-(\delta KV^* + \lambda KV^*) - \sigma KU^*] \\
&-\mathrm{K}U^*(\sigma\alpha + \sigma\beta + \sigma\lambda),
\end{aligned}$$

This provides its characteristic equation.

$$\lambda^3 + a_1\lambda^2 + a_2\lambda + a_3 = 0,$$

where

$$a_1 = (\delta + \alpha + \beta + \mu U^* + kV^*),$$

$a_2 = (kV^*\delta + kV^*\alpha + kV^*\beta + \mu U^*\delta + \alpha\delta - \beta\delta + \beta KV^* - \mathrm{K}U^*\sigma),$
$a_3 = \mu U^*\delta(\alpha + \beta) + kV^*\delta(\alpha + \beta) + \mathrm{K}U^*\sigma\alpha,$
$a_3 = \delta(\alpha + \beta)\{\mu U^* + kV^*\} + \mathrm{K}U^*\sigma\alpha.$
Hence the use of the Routh Hurwitz table it is thus possible to conclude that all the roots of the characteristic equation have a negative real part. This means that the I^* equilibrium point is a locally stable one and approaches a stable state as time elapses.

4. Existence and Uniqueness of the Solution

This part proves that the system has a solution and the solution is unique
Theorem. 4.1 The function G_i for
$i = 1,2,3$ satisfies the Lipschitz and contraction mapping conditions if the following inequality holds: $0 \leq n_i < 1$.
Proof For U and U_1, we have
$\| G_1(t,U) - G_1(t,U_1) \| = \| A - KU(t)V(t) + \beta E(t) - \mu U(t) - A + KU_1(t)V(t) - \beta E(t) + \mu U_1(t) \|,$
$\leq \| -K[U(t) - U_1(t)]V(t) - \mu[U(t) - U_1(t)] - \beta \|,$
$\leq \| KV(t)[U(t) - U_1(t)] \| + \| \mu[U(t) - U_1(t)] \|,$
$\leq [K \| V(t) \| + \mu] \| U(t) - U_1(t) \|,$
$\leq [Ky_3 + \mu] \| U(t) - U_1(t) \| .$
There are positive constant y_1, y_2, y_3 such as
$\| U(t) \| \leq y_1; \| E(t) \| \leq y_2; \| V(t) \| \leq y_3;$
and
$n_1 = ([Ky_3 + \mu])$ are non-negative bounded function.
Hence
$\| G_1(t, U(t)) - G_1(t, U_1) \| \leq n_1 \| (U(t) - U_1(t)) \| .$
similarly, we can prove G_i for $i = 1,2$satisfy the Lipschitz condition.
$\| G_1(t, U(t)) - G_1(t, U_1) \| \leq n_1 \| (U(t) - U_1(t)) \| .$
$\| G_2(t, E(t)) - G_2(t, E_1) \| \leq n_2 \| (E(t) - E_1(t)) \| .$
$\| G_3(t, V(t)) - G_3(t, V_1) \| \leq n_3 \| (V(t) - V_1(t)) \| .$
Consequently, the Lipschitz condition is satisfied by G_i. Additionally, the function is contraction under the constraint $0 \leq n_i < 1$. Take into account the following recursive forms, depending on the system:

$$U_r(t) = \frac{1}{\Gamma(\upsilon)}\int_0^t (t-m)^{\upsilon-1} G_1(m, U_{r-1})\,dm,$$

$$E_r(t) = \frac{1}{\Gamma(\upsilon)}\int_0^t (t-m)^{\omega-1} G_2(m, E_{r-1})\,dm,$$

$$V_r(t) = \frac{1}{\Gamma(\omega)}\int_0^t (t-m)^{\omega-1} G_3(m, V_{r-1})\,dm,$$

The difference between two terms:

$$\Psi_{1r}(t) = U_r(t) - U_{r-1}(t) = \frac{1}{\Gamma(\omega)}\int_0^t (t-m)^{\omega-1}\left(G_1(m, U_{r-1}) - G_1(t, U_{r-2})\right)dm,$$

$$\Psi_{2r}(t) = E_r(t) - E_{r-1}(t) = \frac{1}{\Gamma(\omega)}\int_0^t (t-m)^{\omega-1}\left(G_2(m, E_{r-1}) - G_2(t, E_{r-2})\right)dm,$$

$$\Psi_{3r}(t) = V_r(t) - V_{r-1}(t) = \frac{1}{\Gamma(\omega)}\int_0^t (t-m)^{\omega-1}\left(G_3(m, V_{r-1}) - G_3(t, V_{r-2})\right)dm,$$

Using the initial condition $U(t) = U(0)$,$E(t) = E(0)$,$V(t) = V(0)$. We proceed with the first equation of the aforementioned method based on the norm and the Lipschitz condition and obtain

$\| \Psi_{1r}(t) \| = \| U_r(t) - U_{r-1}(t) \| = \| \frac{1}{\Gamma(\omega)} \int_0^t (t-m)^{\omega-1} (G_1(m, U_{r-1}) - G_1(t, U_{r-2})) \, dm \|,$

$\leq \frac{1}{\Gamma(\omega)} \int_0^t \| (t-m)^{\omega-1} (G_1(m, U_{r-1}) - G_1(t, U_{r-2})) \| \, dm,$

$\| \Psi_{1r}(t) \| \leq \frac{1}{\Gamma(\omega)} \int_0^t \| \Psi_{1(r-1)} \left((t-m)^{\omega-1} \right) \| \, dm.$

We get

$\| \Psi_{2r}(t) \| \leq \frac{n_2}{\Gamma(\omega)} \int_0^t \| \Psi_{1(r-1)} \left((t-m)^{\omega-1} \right) \| \, dm.$

$\| \Psi_{3r}(t) \| \leq \frac{n_3}{\Gamma(\omega)} \int_0^t \| \Psi_{1(r-1)} \left((t-m)^{\omega-1} \right) \| \, dm.$

Then we can write that

$U_r(t) = \sum_{i=1}^r \Psi_{1i}(t); E_r(t) = \sum_{i=1}^r \Psi_{2i}(t); V_r(t) = \sum_{i=1}^r \Psi_{3i}(t).$

We then show that there exists a solution to this problem.

Theorem.4.2 If there exists $t_1 > 1$ such that $\frac{n_i}{\Pi(\omega)} t_{1 \leq} 1$, for $i = 1,2,3$ then there exists at least one solution of the unemployment system (1).

Proof Suppose their exist t such that $\frac{n_i}{\Pi(\omega)} t_{1 \leq} 1$.

$\| \Psi_{1r}(t) \| \leq \frac{n_1}{\Gamma(\omega)} \int_0^t \| \Psi_{1(r-1)} \left((t-m)^{\omega-1} \right) \| \, dm.$

Replacing r by$r-1$ in the above inequility

$\| \Psi_{r-1}(t) \| \leq \left(\frac{n_1}{\Gamma(\omega)} \right) \int_0^t \| \Psi_{1(r-2)} \left((t-m)^{\omega-1} \right) \| \, dm,$

$\leq \left(\frac{n_1}{\Gamma(\omega)} \right)^2 \int_0^t \| \Psi_{1(r-2)} \left((t-m)^{\omega-1} \right) \| \, dm.$

Again replacing r by $r-2$ in the given inequality

$\| \Psi_{r-2}(t) \| \leq \left(\frac{n_1}{\Gamma(\omega)} \right) \int_0^t \| \Psi_{1(r-3)} \left((t-m)^{\omega-1} \right) \| \, dm,$

$\leq \left(\frac{n_1}{\Gamma(\omega)} \right)^3 \int_0^t \| \Psi_{1(r-3)} \left((t-m)^{\omega-1} \right) \| \, dm.$

If so, if we substitute in this manner repeatedly and employ the initial condition, we get

$\| \Psi_{1r}(t) \| \leq \| U_r(0) \| \left[\frac{r_1}{\Gamma(\omega)} t \right]^r.$

Similarly,we get

$\| \Psi_{2r}(t) \| \leq \| E_r(0) \| \left[\frac{r_1}{\Gamma(\omega)} t \right]^r.$

$\| \Psi_{3r}(t) \| \leq \| V_r(0) \| \left[\frac{r_1}{\Gamma(\omega)} t \right]^r.$

This system has a solution, so it is also continuous. We will prove that $\Psi_{1r}(t)$ $\Psi_{2r}(t)$ $\Psi_{3r}(t)$ converge to system of solution.

Assume $\mathrm{T}_{1r}(t), \mathrm{T}_{2r}(t), \mathrm{T}_{3r}(t)$ as a Fixed point iteration method so that

$U(t) - U(0) = U_r(t) - \mathrm{T}_{1r}(t),$

$E(t) - E(0) = E_r(t) - \mathrm{T}_{2r}(t)$

$V(t) - V(0) = V_r(t) - \mathrm{T}_{3r}(t),$

When we apply the triangle inequality to the Lipschitz $G1$ condition, we obtain: We apply the norm to the first equation of the previous technique, and by applying the Lipschitz condition, we obtain

$\| \mathrm{T}_{1r}(t) \| = \| \frac{1}{\Gamma(\omega)} \int_0^t (G_1(m, U_r) - G_1(t, U_{r-1})) dm \|,$

$\leq \frac{1}{\Gamma(\omega)} \int_0^t (G_1(m, U_r) - G_1(t, U_{r-1})) dm,$

$\leq \frac{1}{\Gamma(\omega)} r_1 \| U_1 - U_{r-1} \| t$

Recursively using the aforementioned procedure, we get

$\| T_{1r}(t) \| \leq \left[\frac{r_1}{\Gamma(\omega)}t\right]^{r+1} m.$
The Lipschitz constant in this case is m. Consequently, the sequence is valid and satisfies the stated requirements as
$\| T_{2r}(t) \| \to 0$; $\| T_{3r}(t) \| \to 0$; as $r \to \infty$.
$\| U_{r+n}(t) - U_r(t) \| \leq \sum\limits_{i=r+1}^{r+n} X_1^i = \frac{X_1^{r+1} - X_1^{r+n+1}}{1 - X_1},$
$\| E_{r+n}(t) - E_r(t) \| \leq \sum\limits_{i=r+1}^{r+n} X_2^i = \frac{X_1^{r+1} - X_2^{r+n+1}}{1 - X_2},$
$\| V_{r+n}(t) - V_r(t) \| \leq \sum\limits_{i=r+1}^{r+n} X_3^i = \frac{X_1^{r+1} - X_3^{r+n+1}}{1 - X_3}.$
By hypothesis $\frac{n_1}{\Gamma(\omega)}t_1 \leq 1.U,E,V$ are Cauchy sequences. Because of this, it is possible to conclude that they are uniformly convergent. This means that the only solution to the fractional system is the limit of the sequences.
Theorem.4.3 If the condition $\left(1 - \frac{n_1}{\Gamma(\omega)}t\right) > 0$, for $i = 1, 2, 3$, holds then the UEV model of unemployment probleming is unique solution.
Proof We suppose that another solution is possible for the system to distinguish the uniqueness of the solution, for instance, $U_1(t), E_1(t), V_1(t)$.
$U(t) - U_1(t) \leq \frac{1}{\Gamma(\omega)} \int\limits_0^t (G_1(m,U) - G_1(m,U_1))dm.$
Now, we take the norm of above equation
$\| U(t) - U_1(t) \| \leq \frac{1}{\Gamma(\omega)} \int\limits_0^t (G_1(m,U) - G_1(m,U_1)) \| dm.$

$$\leq \frac{1}{\Gamma(\omega)} \int\limits_0^t \| (G_1(m,U) - G_1(m,U_1)) \| dm.$$

As per the Lipschitz condition it can be concluded that
$\| U(t) - U_1(t) \| \leq \frac{1}{\Gamma(\omega)} n_1 t \int\limits_0^t \| (U(t) - U_1(t)) \| dm,$
consequently
$\| U(t) - U_1(t) \| - \frac{1}{\Gamma(\omega)} n_1 t \| (U(t) - U_1(t)) \| \leq 0,$

$$\| U(t) - U_1(t) \| \left[1 - \frac{1}{\Gamma(\omega)} n_1 t\right] \| \leq 0. \tag{2}$$

If $1 - \frac{1}{\Gamma(\omega)}t > 0$, then the previous Eq. (2) has the form
$\| U(t) - U_1(t) \| = 0.$
Accordingly, $U(t) = U_1(t)$. Use the same method for all solutions for
$i = 1, 2, 3,$, and we obtain
$\| E(t) - E_1(t) \| = 0; \| V(t) - V_1(t) \| = 0;$
This proves the theorem. □

5. Hyers-Ulam-Rassias Stability

Hyers-Ulam-Rassias stability is a property of a functional equation in that they suffer arbitrary small perturbations in their arguments. It is an easily understood concept in functional analysis, especially in the theory of functional equations. This measures the closeness of a solution, of a functional equation to a solution of the next functional equation that will be studied. This means that it doesnt matter in which part of the equation formulas containing the knowns and unknowns are arranged because, for applications in which the time derivation of the unknowns is equal to 0 to obtain the steady-state solutions, these equations are stable. This can be used in practice in practically all branches of mathematics, physics, engineering, and economics to mention but a few. Let us write the model as follows:

$$\begin{cases} {}_0^cD_t^{\omega}\left[\xi\left(t\right)\right] = \Delta\left(t,\xi\left(t\right)\right), \\ \xi\left(0\right) = \xi_0, 0 < t < T < \infty, \end{cases} \tag{3}$$

where $\xi = \{U,E,V\}$ and $\Delta = (\Delta_1,\Delta_2,\Delta_3)$ is a continuous vector function.

Definition 5.1. *Assume that the fractional order ω is $0<\omega<1$ and $F:[0,T]\times R^3 \to R^3$ is a continuous mapping. Then, model (3) is Hyers-Ulam stable if $\exists$ $\varsigma>0$ and $\mathrm{P}>0$, such that for each solution $\xi \in \mathrm{O}\left([0,T],R^3\right)$, the following inequality exists:*
$\| {}_0^cD_t^{\omega}[\xi] - \Delta(t,\xi) \| \leq \mathrm{P}$,

$$\forall t \in [0,T]$$

$\exists$ a solution $\xi' \in \mathrm{O}\left([0,T],R^3\right)$ of model (3), such as

$$\| \xi - \xi' \| \leq \varsigma \mathrm{P}, \forall t \in [0,T]. \tag{4}$$

.

Definition 5.2. *The fractional-order ω is assumed to be $0<\omega<1$. These functions are continuous mappings: $\Delta:[0,T]\times R^3 \to R^3$ and $\Theta:[0,T]\to R^+$. Accordingly, model (3) is generalized Hyers-Ulam-Rassias stable with respect to Θ if $\exists$ $\mathrm{O}_{\Delta,\Theta}>0$, so that for any solution $\xi \in \mathrm{O}\left([0,T],R^3\right)$, the following inequality holds:*

$$\| {}_0^cD_t^{\omega}\left[\xi\left(t\right)\right] - \Delta\left(t,\xi\left(t\right)\right) \| \leq \Theta\left(t\right), \forall t \in [0,T] \tag{5}$$

$\exists \xi' \in \mathrm{O}\left([0,T],R^3\right)$ of model (3), such as

$$\| \xi - \xi' \| \leq \mathrm{O}_{\Delta,\Theta}\Theta\left(t\right) \forall t \in [0,T] \tag{6}$$

Now, to prove that model (3) is the Hyers-Ulam-Rassias stable, we assume that:
• $[L_1]$ $\Delta:[0,T]\times R^3 \to R^3$ *is a continuous mapping.*
• $[L_2]$ $\exists \mathrm{O}_\Delta > 0$ *such that for each solution* $\xi,\xi', \in \mathrm{O}\left([0,T],R^3\right)$,
$\| \xi - \xi' \| \leq \mathrm{O}_\Delta \| \xi - \xi' \|, \forall t \in [0,T]$.
• $[L_3]$ *Let* $\Theta \in ([0,T],R^+)$ *be an increasing mapping, and let* $\mathrm{M}_{\Theta>0,}$ *such that*
$\int_0^t \Theta(\eta)\, d\eta \leq \mathrm{M}_\Theta \Theta(t), \forall t \in [0,T]$

Theorem.5.1 It is assumed that $[L_1]-[L_3]$ exists, and model (3) is of the generalized Hyers-Ulam-Aghalary type.Rassias is stable with respect to Θ on the interval provided that $\Omega(\omega)\mathrm{O}_\Delta < 0$table with respect to Θ on the interval as long as $\Omega(\omega)\mathrm{O}_\Delta < 0$.
Proof Let $\xi \in \mathrm{O}\left([0,T],R^3\right)$ be a solution of model (3). Then, the unique solution of model (3) from Theorem (4.3) is

$$\xi = \xi\left(0\right) + \Omega(\omega)\Delta(t,\Omega') + \Omega(\omega)\int_0^t \Delta\left(\xi,\xi\left(\eta\right)\right) d\eta. \tag{7}$$

On the evidence of (5), we can say that
$\| \xi' - \xi\left(0\right) + \Omega(\omega)\Delta(t,\Omega) + \sigma(\omega)\int_0^t \Delta(\xi,\xi(\eta))\, d\eta \|$

$\leq \Omega(\omega)\Theta(t)+\sigma(\omega)\int\limits_0^t \Theta(\eta)d\eta$
$\leq (\Omega(\omega)+\sigma(\omega)\mathrm{M}_\Theta)\Theta(t)$.
So,
$\| \xi-\xi' \| \leq \| \xi'-\xi(0)-\Omega(\omega)\Delta(t,\Omega')-\sigma(\omega)\int\limits_0^t \Delta(\eta,\xi'(\eta))d\eta \|$

$\| \xi'-\xi(0)-\Omega(\omega)\Delta(t,\Omega')-\sigma(\omega)\int\limits_0^t \Delta(\eta,\xi(\eta))d\eta$

$-\Omega(\omega)\Delta(t,\Omega')-\sigma(\omega)\int\limits_0^t \Delta(\eta,\xi'(\eta))d\eta$

$+\Omega(\omega)\Delta(t,\Omega')-\sigma(\omega)\int\limits_0^t \Delta(\eta,\xi'(\eta))d\eta \|$

$\leq \| \xi'-\xi(0)-\Omega(\omega)\Delta(t,\xi')-\sigma(\omega)\int\limits_0^t \Delta(\eta,\xi(\eta))d\eta \|$

$+\Omega(\omega) \| \Delta(t,\xi)-\Delta(t,\xi') \| +\sigma(\omega\int \| (\eta,\xi(\eta))-\Delta(\eta,\xi'(\eta)) \| d\eta$

$\leq (\Omega(\omega)+\sigma(\omega)\mathrm{M}_\Theta)\Theta(t)+\Omega(\omega)\mathrm{O}_\Delta \| \xi-\xi' \| +\Theta(\omega)\mathrm{O}_\Delta\int\limits_0^t \| \xi(\eta)-\xi'(\eta) \| d\eta$
Now, $\xi(\omega)\mathrm{O}_\Delta < 1$, So

$$\| \xi-\xi' \| \leq \frac{(\Omega(\omega)+\sigma(\omega)\mathrm{M}_\Theta)\Theta(t)}{1-\Omega(\omega)\mathrm{O}_\Delta}+\frac{\sigma(\omega)\mathrm{O}_\Delta}{1-\Omega(\omega)\mathrm{O}_\Delta}\int\limits_0^t \| \xi(\eta)-\xi'(\eta) \| d\eta \tag{8}$$

The Gronwalls inequality yields

$$\| \xi-\xi' \| \leq \left[\frac{(\Omega(\omega)+\sigma(\omega)\mathrm{M}_\Theta)}{1-\Omega(\omega)\mathrm{O}_\Delta}\exp(t)\right]\sigma(t) \tag{9}$$

On setting $\mathrm{O}_{\Delta,\Theta}=\left[\frac{(\Omega(\omega)+\sigma(\omega)\mathrm{M}_\Theta)}{1-\Omega(\omega)\mathrm{O}_\Delta}\exp(t)\right]$, We have

$$\| \xi-\xi' \| \leq \mathrm{O}_{\Delta,\Theta}\mathrm{O}(t). \tag{10}$$

Inequality (10) authenticated that model (3) is generalized HyersUlam-Rassias stable concerning Θ.

6. Numerical Scheme

We establish a numerical scheme for the proposed model (1). The following is a system of Caputo fractional differential equation.

$$\begin{array}{l} {}_0^CD_t^\omega U(t)=\mathrm{H}_1(t,U), \\ {}_0^CD_t^\omega E(t)=\mathrm{H}_2(t,U), \quad , \\ {}_0^CD_t^\omega V(t)=\mathrm{H}_3(t,U) \end{array} \tag{11}$$

where

$$A-KU(t)V(t)+\beta E(t)-\mu U(t)=\mathrm{H}_1(t,U),$$
$$KU(t)V(t)-\beta E(t)-\alpha E(t)=\mathrm{H}_2(t,E),$$
$$\sigma U(t)-\delta V(t)=\mathrm{H}_3(t,V).$$

We consider the first equation of system (11) and apply the Caputo integral we have

$$U(t)-U(0)=\frac{1-\omega}{\Gamma(\omega)}\int\limits_0^t \mathrm{H}_1(\varepsilon,U(\varepsilon))(t-\varepsilon)^{\omega-1}d\varepsilon. \tag{12}$$

We can write the following at point $\gamma_{\vartheta+1} = (\vartheta+1)\Delta t$:

$$U(t_{\vartheta+1}) - U(0) = \frac{1-\omega}{\Gamma(\omega)} \int_0^{t_{\vartheta+1}} \mathrm{H}_1(\varepsilon, U(\varepsilon))(t_{\vartheta+1}-\varepsilon)^{\omega-1} d\varepsilon. \tag{13}$$

As a result,

$$U(t_{\vartheta+1}) = U(0) + \frac{1-\omega}{\Gamma(\omega)} \sum_{\kappa=2}^{\vartheta} \int_{t_\kappa}^{t_{\vartheta+1}} \mathrm{H}_1(\varepsilon, U(\varepsilon))(t_{\vartheta+1}-\varepsilon)^{\omega-1} d\varepsilon. \tag{14}$$

Using the Newton polynomial, we obtain

$$\left\{ \begin{array}{l} U\left(t^{\mathrm{K}+1}\right) = U_0 + \frac{1-\omega}{\gamma(\omega)} \sum\limits_{\kappa=2}^{\vartheta} \int\limits_{t_\kappa}^{t_{\kappa+1}} \left\{ \begin{array}{l} \mathrm{H}_1\left(t_{\kappa-2,} U^{\kappa-2}\right) + \frac{\mathrm{H}_1\left(t_{\kappa-1,} U^{\kappa-1}\right) - \mathrm{H}_1\left(t_{\kappa-2,} U^{\kappa-2}\right)}{\Delta t}(\varepsilon - t_{\kappa-2}) + \\ \frac{\mathrm{H}_1(t_{\kappa,} U^{\kappa}) - 2\mathrm{H}_1\left(t_{\kappa-1,} U^{\kappa-1}\right)\left(\mathrm{H}_1\left(t_{\kappa-2,} U^{\kappa-2}\right)\right)}{2(\Delta t)^2} \times (\varepsilon - t_{\kappa-2})(\varepsilon - t_{\kappa-1}) \end{array} \right\} \\ \times (t_{\kappa+1} - \varepsilon)^{\omega-1} d\varepsilon. \end{array} \right. \tag{15}$$

As a result,

$$U\left(t^{\mathrm{K}+1}\right) = U_0 + \frac{1-\omega}{\Gamma(\omega)} \sum_{\kappa=2}^{\vartheta} \left\{ \begin{array}{l} \int\limits_{t_\kappa}^{t_{\mathrm{K}+1}} \mathrm{H}_1\left(t_{\kappa-2,} U^{\kappa-2}\right)(t_{\kappa+1}-\varepsilon)^{\omega-1} d\varepsilon \\ + \int\limits_{t_\kappa}^{t_{\mathrm{K}+1}} \frac{\mathrm{H}_1\left(t_{\kappa-1,} U^{\kappa-1}\right) - \mathrm{H}_1\left(t_{\kappa-2,} U^{\kappa-2}\right)}{\Delta t} \\ (\varepsilon - t_{\kappa-2})(t_{\kappa+1}-\varepsilon)^{\omega-1} d\varepsilon \\ + \int\limits_{t_\kappa}^{t_{\mathrm{K}+1}} \begin{array}{c} \frac{\mathrm{H}_1(t_{\kappa,} U^{\kappa}) - 2\mathrm{H}_1\left(t_{\kappa-1,} U^{\kappa-1}\right)\left(\mathrm{H}_1\left(t_{\kappa-2,} U^{\kappa-2}\right)\right)}{2(\Delta t)^2} \\ (\varepsilon - t_{\kappa-2})(\varepsilon - t_{\kappa-1})(t_{\kappa+1}-\varepsilon)^{\omega-1} d\varepsilon \end{array} \end{array} \right\} \tag{16}$$

$$\times (t_{\kappa+1}-\varepsilon)^{\omega-1} d\varepsilon.$$

Consequently,

$$\begin{aligned} U\left(t^{\mathrm{K}+1}\right) = {} & U_0 + \frac{1-\omega}{\Gamma(\omega)} \sum_{\mathrm{K}=2}^{\vartheta} \mathrm{H}_1\left(t_{\kappa-2,} U^{\kappa-2}\right) \int_{t_k}^{t_{k+1}} (t_{\kappa+1}-\varepsilon)^{\omega-1} d\varepsilon + \frac{1}{\Gamma(\omega)} \sum_{\mathrm{K}=2}^{\vartheta} \frac{\mathrm{H}_1\left(t_{\kappa-1,} U^{\kappa-1}\right) - \mathrm{H}_1\left(t_{\kappa-2,} U^{\kappa-2}\right)}{\Delta t} \\ & \times \int_{t_k}^{t_{k+1}} (\varepsilon - t_{\kappa-2})(t_{\kappa+1}-\varepsilon)^{\omega-1} d\varepsilon \\ & + \frac{1}{\Gamma(\omega)} \sum_{\mathrm{K}=1}^{\vartheta} \frac{\mathrm{H}_1(t_{\kappa,} U^{\kappa}) - 2\mathrm{H}_1\left(t_{\kappa-1,} U^{\kappa-1}\right)\left(\mathrm{H}_1\left(t_{\kappa-2,} U^{\kappa-2}\right)\right)}{2(\Delta t)^2} \\ & \times \int_{t_k}^{t_{k+1}} (\varepsilon - t_{\kappa-2})(\varepsilon - t_{\kappa-1})(t_{\kappa+1}-\varepsilon)^{\omega-1} d\varepsilon. \end{aligned} \tag{17}$$

We get

$$
\begin{aligned}
&U^{\vartheta+1}=U_0+\tfrac{(\Delta t)^{\omega}}{\Gamma(\omega+1)}\sum_{k=1}^{\vartheta}\mathrm{H}_1\left(t_{\mathrm{K}-2,}U^{k-2}\right)\times\left[(\vartheta-\mathrm{K}+1)^{\omega}-(\vartheta-\mathrm{K})^{\omega}\right]\\
&+\tfrac{(\Delta t)^{\omega}}{\Gamma(\omega+2)}\sum_{k=2}^{\vartheta}\mathrm{H}_1\left(t_{k-1,}U^{k-1}\right)-\left(t_{\mathrm{K}-2,}U^{k-2}\right)\\
&\times\left[\begin{array}{l}(\vartheta-\mathrm{K}+1)^{\omega}(\vartheta-\mathrm{K}+3+2\omega)\\-(\vartheta-\kappa)^{\omega}(\vartheta-\mathrm{K}+3+3\omega)\end{array}\right]\\
&\times+\tfrac{(\Delta t)^{\omega}}{2\Gamma(\omega+3)}\sum_{k=2}^{\vartheta}\left[\mathrm{H}_1\left(t_{k,}U^{k}\right)-2\mathrm{H}_1\left(t_{k-1,}U^{k-1}\right)+\left(\mathrm{H}_1\left(t_{k-2,}U^{k-2}\right)\right)\right]\\
&\times\left[\begin{array}{l}(\vartheta-\mathrm{K}+1)^{\omega}\left[\begin{array}{l}2(\vartheta-\mathrm{K})^{2}+(3\omega+10)(\vartheta-\mathrm{K})\\+2\omega^{2}+9\omega+12\end{array}\right]\\-(\vartheta-\mathrm{K})^{\omega}\left[\begin{array}{l}2(\vartheta-\mathrm{K})^{2}+(5\omega+10)(\vartheta-\kappa)\\+6\omega^{2}+18\omega+12\end{array}\right]\end{array}\right]
\end{aligned}
\tag{18}
$$

Similarly from the second, third, and fourth equations of the system (11), we can write

$$
\begin{aligned}
&E^{\vartheta+1}=E_0+\tfrac{(\Delta t)^{\omega}}{\Gamma(\omega+1)}\sum_{k=2}^{\vartheta}\left(\mathrm{H}_2\left(t_{k-2,}E^{k-2}\right)\right)\left[(\vartheta-\mathrm{K}+1)^{\omega}-(\vartheta-\mathrm{K})^{\omega}\right]\\
&+\tfrac{(\Delta t)^{\omega}}{\Gamma(\omega+2)}\sum_{k=2}^{\vartheta}\left[\left(\mathrm{H}_2\left(t_{k-2,}E^{k-2}\right)\right)-\left(\mathrm{H}_2\left(t_{k-2,}E^{k-2}\right)\right)\right]\\
&\times\left[\begin{array}{l}(\vartheta-\mathrm{K}+1)^{\omega}(\vartheta-\mathrm{K}+3+2\omega)\\-(\vartheta-\mathrm{K})^{\omega}(\vartheta-\mathrm{K}+3+3\omega)\end{array}\right]\\
&+\tfrac{(\Delta t)^{\omega}}{2\Gamma(\omega+3)}\sum_{k=2}^{\vartheta}\left[\begin{array}{l}\left(\mathrm{H}_2\left(t_{k,}E^{k}\right)\right)-2\mathrm{H}_2\left(t_{k-1,}E^{k-1}\right)\\+\mathrm{H}_2\left(t_{k-2,}E^{k-2}\right)\end{array}\right]\\
&\times\left[\begin{array}{l}(\vartheta-\mathrm{K}+1)^{\omega}\left[\begin{array}{l}2(\vartheta-\mathrm{K})^{2}+(3\omega+10)(\vartheta-\mathrm{K})\\+2\omega^{2}+9\omega+12\end{array}\right]\\-(\vartheta-\mathrm{K})^{\omega}\left[\begin{array}{l}2(\vartheta-\mathrm{K})^{2}+(5\omega+10)(\vartheta-\mathrm{K})\\+6\omega^{2}+18\omega+12\end{array}\right]\end{array}\right],
\end{aligned}
\tag{19}
$$

and

$$
\begin{aligned}
&V^{\vartheta+1}=V_0+\tfrac{(\Delta t)^{\omega}}{\Gamma(\omega+1)}\sum_{k=2}^{\vartheta}\left(\mathrm{H}_3\left(t_{k-2,}V^{k-2}\right)\right)\left[(\vartheta-\mathrm{K}+1)^{\omega}-(\vartheta-\mathrm{K})^{\omega}\right]\\
&+\tfrac{(\Delta t)^{\omega}}{\Gamma(\omega+2)}\sum_{k=2}^{\vartheta}\left[\left(\mathrm{H}_3\left(t_{k-2,}V^{k-2}\right)\right)-\left(\mathrm{H}_3\left(t_{k-2,}V^{k-2}\right)\right)\right]\\
&\times\left[\begin{array}{l}(\vartheta-\mathrm{K}+1)^{\omega}(\vartheta-\mathrm{K}+3+2\omega)\\-(\vartheta-\mathrm{K})^{\omega}(\vartheta-\mathrm{K}+3+3\omega)\end{array}\right]\\
&+\tfrac{(\Delta t)^{\omega}}{2\Gamma(\omega+3)}\sum_{k=2}^{\vartheta}\left[\begin{array}{l}\left(\mathrm{H}_3\left(t_{k,}V^{k}\right)\right)-2\mathrm{H}_3\left(t_{k-1,}V^{k-1}\right)\\+\mathrm{H}_3\left(t_{k-2,}V^{k-2}\right)\end{array}\right]\\
&\times\left[\begin{array}{l}(\vartheta-\mathrm{K}+1)^{\omega}\left[\begin{array}{l}2(\vartheta-\mathrm{K})^{2}+(3\omega+10)(\vartheta-\mathrm{K})\\+2\omega^{2}+9\omega+12\end{array}\right]\\-(\vartheta-\mathrm{K})^{\omega}\left[\begin{array}{l}2(\vartheta-\mathrm{K})^{2}+(5\omega+10)(\vartheta-\mathrm{K})\\+6\omega^{2}+18\omega+12\end{array}\right]\end{array}\right].
\end{aligned}
\tag{20}
$$

7. Numerical Simulation

In this subsection, we examine the numerical results and analysis for the Caputo unemployment model (1) to demonstrate how fractional calculus can enhance unemployment dynamics modeling. Using experimental parameter values from Table 1 and a step size of $h=0.01$, the initial conditions are defined at a positive equilibrium: unemployment $U = 17500$, employment rate $E = 69400$, and vacancy rate $V = 1500$, taken from [6]. The time variable $t = 50$ represents 50 months, allowing a view of both the immediate and extended effects of the model. Figures 1 and 2 depict the dynamics of unemployment ($U(t)$), employment ($E(t)$), and vacancies ($V(t)$) modeled using integer-order derivatives ($\omega = 1$). The fractional order ω represents the memory effect inherent in fractional calculus, where values less than 1 introduce a higher degree of past dependence into system dynamics. When ω is less than 1, the unemployment rate decreases more rapidly, as illustrated in Figures 3, 4, and 5. At these lower values of ω, the model more accurately reflects unemployment dynamics by capturing both short-term reactions and historical influences, which are often significant in real-world scenarios. Lower fractional orders cause the model to respond more dynamically to changes, resulting in a reduction in the number of unemployed and skilled-jobless individuals. On the other hand, larger fractional orders offer a broader and richer perspective of the unemployment dynamics, which became one of the key advantages of introducing fractional derivatives capable of capturing short-term and intricate long-term correlations. A main feature of employing fractional derivatives is that memory effects can be incorporated when the conventional integer-order derivatives cannot. This property applies greatly in unemployment modeling because previous state data influences interactions and policies to make current employment rates. The models provided here show that fractional derivatives are more flexible and realistic than integer-order models in terms of gradual unemployment dynamics. The second batch of tests looks at what happens to the unemployment rate U, the employment rate E, and the vacancy rate V when the job creation rate, σ is varied. As depicted in Figures 6, 7 and 8, a policy that raises σ (creates more jobs) is a strong instrument to combat unemployment. According to the formula of the model when σ is equal to 0.687, this shows the possibility of reducing the unemployment rate to about 7%, which organizations and governments set as their goals of employment. This implies that a job creation rate closely around this frontier level is of significant importance to achieving large changes in unemployment a result that fractional calculus makes visible by examining various forms of change in the employment process, including those based on a memory component.

The graphical comparisons between the classical integer-order model ($\omega = 1$) and fractional-order models ($\omega < 1$) reveal significant differences in system behavior. The integer-order model (Figures 1-2) demonstrates abrupt changes in unemployment ($U(t)$), employment ($E(t)$), and vacancies ($V(t)$) due to its reliance on instantaneous dynamics, which oversimplifies real-world processes. Conversely, the fractional-order models (Figures 3-8) capture smoother transitions and gradual adjustments, reflecting memory effects and historical dependencies inherent in socio-economic systems. These results underscore the ability of fractional calculus to provide a more realistic and nuanced representation of unemployment dynamics, offering deeper insights into long-term policy impacts. The choice of a fractional-order model stems from its ability to account for memory effects and hereditary properties, which are often integral to biological and socio-economic systems. Unlike classical integer-order models that assume instantaneous dynamics, fractional-order models incorporate past influences, providing a more comprehensive understanding of system behavior. For instance, unemployment trends, analogous to biological systems, are influenced by historical factors like prior job creation policies and economic conditions. The fractional-order model reveals how these historical influences shape present dynamics, as shown in Figures 3-8, where lower fractional orders ($\omega < 1$) demonstrate more sensitive and realistic responses. This capacity to model gradual transitions and long-term dependencies highlights the biological and real-world relevance of fractional models, making them superior to integer-order approaches in capturing complex, memory-driven processes.

Table 1: The probable values of parameters in the model for unemployment.

Parameters	Values
A	3000
β	0.01
μ	0.032
α	0.035
δ	0.075
k	1.8×10^{-5}
σ	0.1

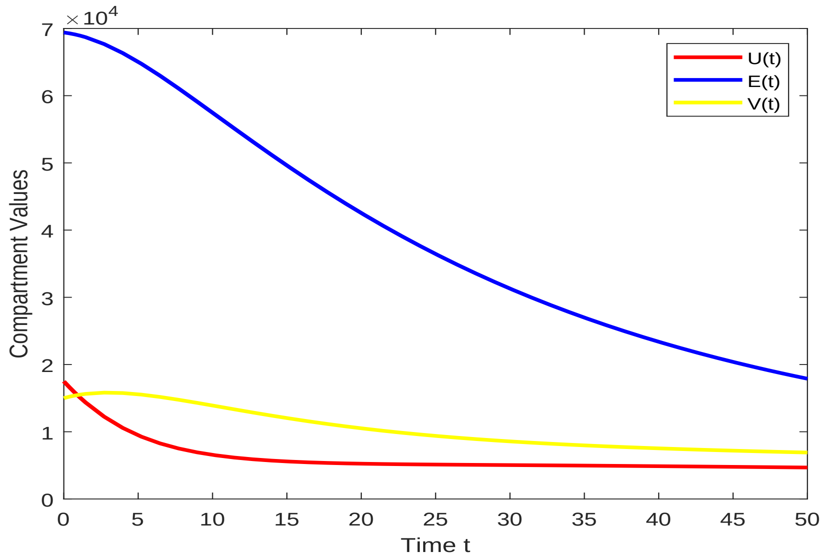

Figure 1: Solution of the classical order system when when $\sigma = 0.1$.

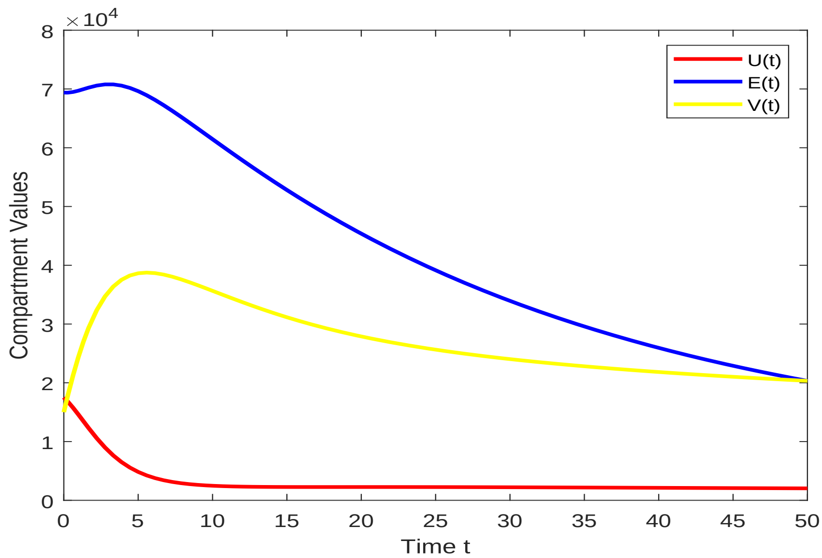

Figure 2: Solution of the classical order system when when $\sigma = 0.687$.

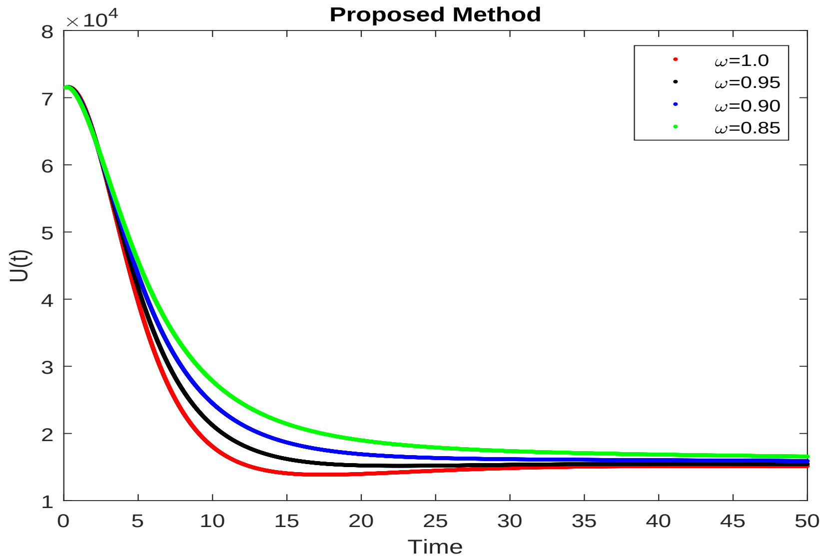

Figure 3: Simulation of $U(t)$ when $\sigma = 0.1$.

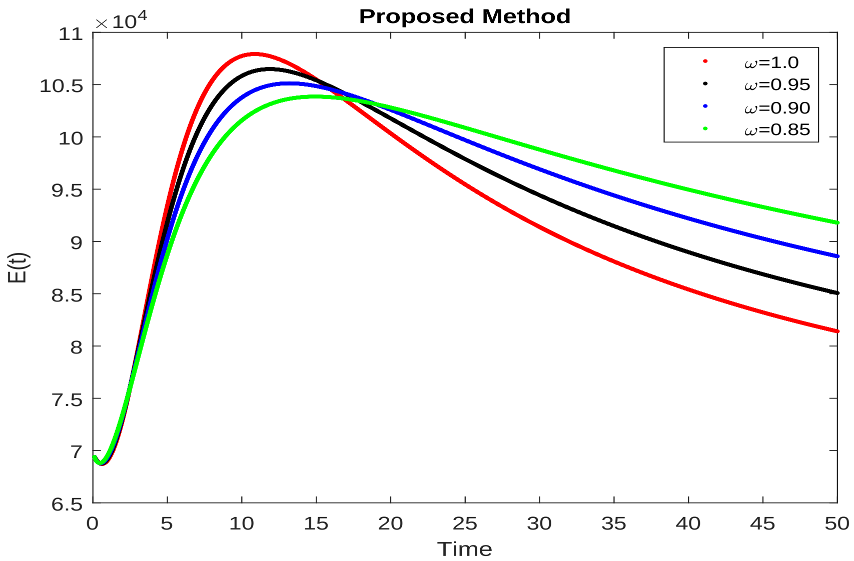

Figure 4: Simulation of $E(t)$ when $\sigma = 0.1$.

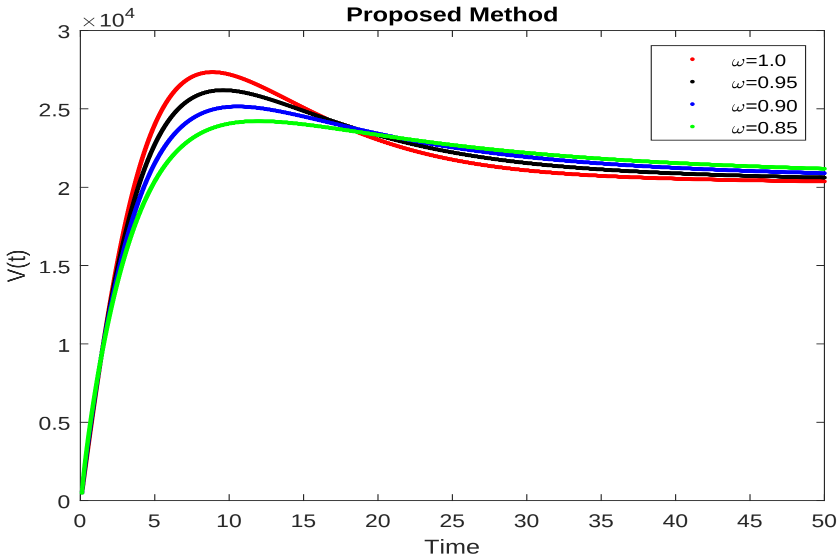

Figure 5: Simulation of $U(t)$ when $\sigma = 0.1$.

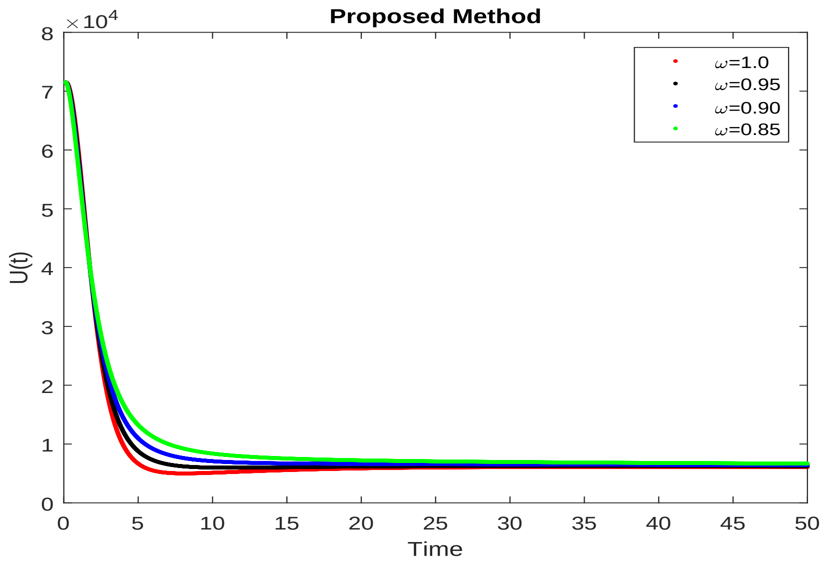

Figure 6: Simulation of $U(t)$ when $\sigma = 0.687$.

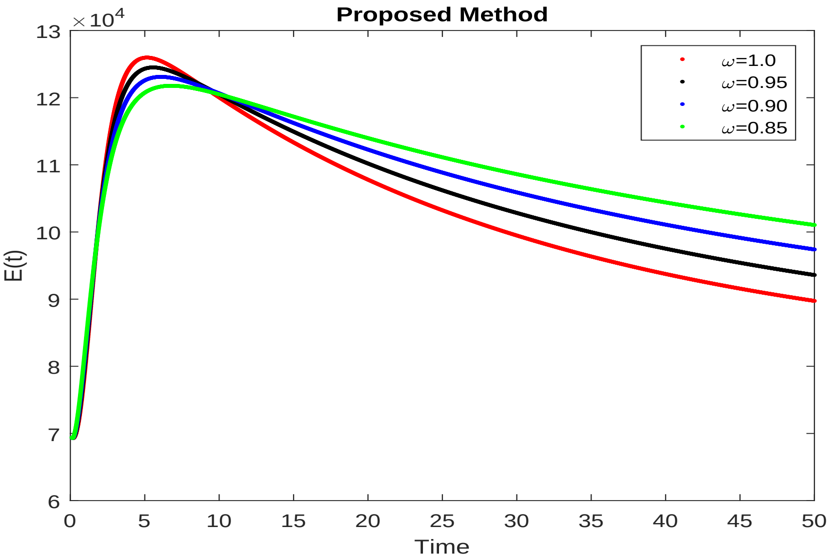

Figure 7: Simulation of $E(t)$ when $\sigma = 0.687$.

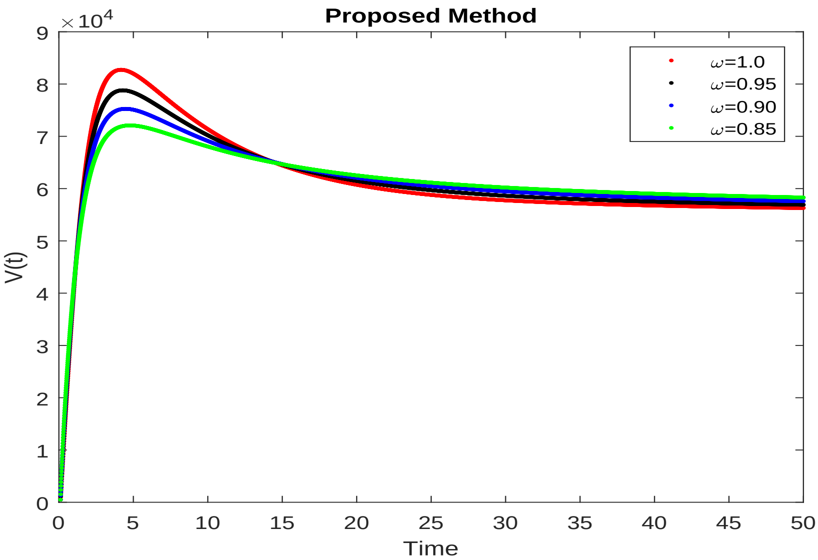

Figure 8: Simulation of $U(t)$ when $\sigma = 0.687$.

8. Conclusion

Unemployment is a persistent global issue that demands sophisticated analytical approaches for effective policy development. This study introduces a fractional-order unemployment model based on the Caputo derivative, offering a significant advantage in capturing memory effects and hereditary dynamics over traditional integer-order models. The graphical comparison of results under various fractional orders (ω) demonstrates the model's robustness and flexibility. For instance, lower fractional orders ($\omega < 1$) reveal enhanced sensitivity to historical unemployment trends, enabling more dynamic responses to policy changes. Conversely, results at higher fractional orders align more closely with integer-order behavior, providing a broader but less nuanced perspective of system dynamics. These visualizations effectively communicate the model's capacity to simulate real-world unemployment scenarios under different assumptions, making the results accessible and actionable for policymakers. Numerical simulations highlight the importance of parameters such as the job creation rate (σ) and fractional order (ω), showing their influence on unemployment stabilization. The inclusion of memory effects through fractional calculus enhances the model's accuracy and relevance, demonstrating its

superiority over traditional methods in understanding gradual system adjustments and the cumulative effects of past policies.
This study underscores the potential of fractional-order models to provide deeper insights into socio-economic systems. The graphical analyses further validate the model's utility, making its outcomes transparent and easily interpretable. Future extensions could incorporate additional factors, such as technological impacts and workforce reskilling, to expand the models applicability to broader socio-economic challenges.

References:

[1] N. T. Feather, The psychological impact of unemployment, Springer Science & Business Media, 2012.

[2] A. H. Goldsmith, J. R. Veum, and W. Darity Jr, The psychological impact of unemployment and joblessness, The J. Socio-Econ. 25 (1996), 333358.

[3] R. Tarling, Unemployment and crime, Home Office Res. Bull. 14 (1982), 2833.

[4] R. L. Jin, C. P. Shah, and T. J. Svoboda, The impact of unemployment on health: a review of the evidence, CMAJ: Canadian Med. Assoc. J. 153 (1995), 529.

[5] S. Sundar, A. Tripathi, and R. Naresh, Does unemployment induce crime in society? a mathematical study, Am. J. Appl. Math. Stat. 6 (2018), 4453.

[6] H. A. Ashi, M. Raneah, Al-Maalwi, and Sarah Al-Sheikh. Study of the unemployment problem by mathematical modeling: Predictions and controls. The Journal of Mathematical Sociology 46, (2022) 301-313.

[7] R. M. Al-Maalwi, H. A. Ashi, and S. Al-sheikh, Unemployment model, Appl. Math. Sci. 12 (2018), 9891006.

[8] S. Al-Sheikh, R. Al-Maalwi, and H. A. Ashi, A mathematical model of unemployment with the effect of limited jobs, Comptes Rendus. Mathematique 359 (2021), 283290.

[9] R. Al-Maalwi, S. Al-Sheikh, H. A. Ashi, and S. Asiri, Mathematical modeling and parameter estimation of unemployment with the impact of training programs, Math. Comput. Simul. 182 (2021), 705720.

[10] A. Atangana, and D. Baleanu . New fractional derivatives with nonlocal and non-singular kernel: theory and application to heat transfer model. arXiv preprint arXiv: (2016) 1602.03408.

[11] B. Maayah, and Arqub, O. A. Hilbert approximate solutions and fractional geometric behaviors of a dynamical fractional model of social media addiction affirmed by the fractional Caputo differential operator. Chaos, Solitons & Fractals: X, 10 (2023), 100092.

[12] B. S. Lassong, M. Dasumani, J. K. Mungatu, and S. E. Moore. Power and MittagLeffler laws for examining the dynamics of fractional unemployment model: A comparative analysis. Chaos, Solitons & Fractals: X, 13, (2024) 100117.

[13] S. Jamil, A. Bariq, M. Farman, K.S. Nisar, A. Akgl, and M.U. Saleem. Qualitative analysis and chaotic behavior of respiratory syncytial virus infection in human with fractional operator. Scientific Reports, 14, (2024), 2175.

[14] A. Zehra, S. Jamil, M. Farman, and K.S. Nisar. Modeling and analysis of Hepatitis B dynamics with vaccination and treatment with novel fractional derivative. Plos one, 19, (2024), e0307388.

[15] S. Jamil, M. Farman, A. Akgl, M. U. Saleem, E. Hincal, E., and S. M. El Din . Fractional order age dependent Covid-19 model: an equilibria and quantitative analysis with modeling. Results in Physics, 53, (2023) 106928.

[16] P. A. Naik, M. Farman, K. Jamil, K. S. Nisar, M. A. Hashmi, and Z. Huang. Modeling and analysis using piecewise hybrid fractional operator in time scale measure for ebola virus epidemics under MittagLeffler kernel. Scientific Reports, 14,(2024), 24963.